JEAS | Journal of Economics and Administrative Sciences
E-ISSN: 2148-1792 P- ISSN: 1302-2024
Volume 3, Supplement Issue 3
www.jeasweb.org

Employing model-reference adaptive system (MRAS) to embed permanent magnet synchronous motor (PMSM) in electric vehicles

*Ayoub Moradi **
Masters, Electrical Engineering - The Power of Electric Machines, Faculty of Engineering, Islamic Azad University, Tabriz, Iran.
**Corresponding Author*

Navid Taghizadegan Kalantari
Associate professor, Electrical Engineering Department, Faculty of Engineering, Azarbaijan Shahid Madani University, Tabriz, Iran,

ABSTRACT
Today, owing to the diminishing energy sources, ever-increasing consumption of fossil fuels and the ensuing environmental pollution, all major industrialized and developing countries highly dedicated to employing state-of-the-art technology and sciences to reduce fossil fuel consumption and air pollution with the purpose alleviating the damage inflicted on the environment. Therefore, designing and selecting the appropriate motor and subsequently using modern control methods for optimizing and developing electric vehicles is of paramount importance. In this study, a permanent magnet synchronous motor (PMSM) with Model-Reference Adaptive System (MRAS) was used as the driving force of electric vehicles. MRAS method is used to reduce the adverse effects of parameter change in speed control of sensor-less PMSM motors based on feed forward voltage estimation (FFVE). The results from simulation in the Simulink environment of MATLAB indicate that the proposed sensor-less method has very good stability at low speeds compared to current conventional methods, such as sliding-mode observer (SMO), under changing parameters.
Key Words: Electric Vehicles, Permanent Magnet, Synchronous Motor, Forward Feed Voltage, Estimation, Reference Model, Adaptive System

Introduction
The decline in oil reserves and the uprise in the price of fossil fuels, and consequently the increase in urban pollution, have led to a reinvigorated interest in novel types of vehicles, especially electric vehicles that use clean fuels [1]. One of the main parts of the propulsion system in an electric car is its electric motor. Therefore, for optimal performance of an electric vehicle, it is of critical importance to employ an engine with appropriate characteristics. A suitable motor must have special features, the most important of which are high torque and power density, high speed variation range, high efficiency in all parts of the characteristic speed torque, having a wide constant power range, high reliability, low noise and reasonable

price [2]. Therefore, one of the most important points in the design and construction of engines and converters employed in these vehicles is to maintain maximum efficiency at different speeds. In this regard, brushless permanent magnet motors such as permanent magnet synchronous motors (PMSP) have the highest efficiency, and induction motors and reluctance switches are in the next level, and DC motors have the lowest efficiency. Today, with the breakthroughs in the field of permanent magnet motors, brushless permanent magnet motors along with induction motors are the most extensively used and most apt motors on the market for use in electric vehicles. High energy density, high efficiency and high reliability are the most important features of these motors along with limitations such as high manufacturing costs owing to the shortage of permanent magnetic materials and their vulnerability [3].

Permanent magnet brushless motors PMBLs are divided into BLDC and BLAC motors based on the shape of the counter-electromotive voltage in idle mode and current consumption. The most important feature of PMSM is its high efficiency, which is obtained as the ratio of input power to input power after calculating losses. There is no rotor current in the PMSM. The PMSM also has various advantages over other types of AC machines used as servo drives. Among other things, the stator current of an induction motor (IM) consists of two components, namely a magnet and a torque-producing component. The adoption of a permanent magnet on the rotor removes the need to feed the magnetizing current through the stator with the purpose of generating a constant airflow flow, and thus the required stator current is used exclusively to generate electromagnetic. Therefore, with the same output ratio, the PMSM will operate at a higher power factor (owing to the reduced magnetizing component) and, thus, will be highly more efficient than induction motors. The ability to control and quickly change the speed of PMSM motors in a self-controlled manner and the possibility of achieving performance with variable speed over a wide range has led to the provision of various control methods depending on the application of the motor. Controllers of this type of motors play a very important and vital role in controlling the speed and position of the motor. According to the above description, the existence of a suitable control system with high efficiency and reliability and resistant to factors such as model uncertainty, variable parameters of time, disturbances and unknown noise in various applications of the engine, especially in electric vehicles, is essential.

In most sensor-less control methods based on back-EMF, the PMSM steady-state model is considered as a reference. Therefore, no stability is achieved when parameter mismatch and loading conditions change during zero and low speed zone performance [4].

Model-reference adaptive system (MRAS) is one of the most efficient sensor-less control methods and one of the three applied adaptive control methods for controlling PMSMs. Model-reference adaptive system are closed loop control systems that can guarantee system stability. Conventional vector control systems detect motor speed using a speed sensor, but such sensors increase system costs while reduce its capability. Therefore, in recent years, the speed and position of the sensor-less control system has received widespread attention. The key to sensor-less vector control is the correct speed estimation and the model-reference adaptive system is a speed detection method, which can guarantee the stability of the system and reduce the error signal down to negligible through the adaptive parameter setting method, after the deployment of which the estimated speed would become highly accurate. Multi-parameter online identification of PMSM under maximum torque per ampere (MTPA) has been proposed having in mind the inverter voltage disturbance in [5], in which three motor parameters, namely winding resistance and inductance and rotor flux are estimated. To improve the estimation accuracy of this method, including estimating offline and online voltage-source inverter (VSI), both are combined with the d-axis current injection method. This system is complicated by the use of several methods, independent of the motor parameters and the parameters of the switching device. Furthermore, signal injection is used in the estimation process in which acoustic noise is unavoidable. In [6], a multi-parameter estimation method is proposed which has two affine projection algorithms (APA), one for predicting stator dq inductances and the other for predicting stator resistance, rotor flux-linkage and load torque. They also include MTPA-enabled adaptive PI controllers for the internal PMSM drive with the aim of providing more dynamic and highly stable performance. Therefore, this method needs to reset the gain subject to speed changes due to uncertainty in the mechanical parameters. Moreover, the discretization error and the solution to this problem are not stated. Recently, an adaptive observer in the static reference framework [7] has been proposed for sensor-less control of a

permanent magnet synchronous motor with the aim of simultaneously estimating stator inductance, stator resistance and load torque. These parameters are accurately estimated, but the proposed method performs poorly in estimating machine parameters when faced with uncertainty. An adaptive parameter estimation method obtained through a modified sliding mode observer method to achieve convergence in finite time and an online review of alternative permanent excitation (PE) conditions and control of nonlinear robotic systems based on parameter estimation errors is proposed in [8].

The performance of the induction motor was examined considering variations of stator resistance in [9]. The stator resistance is adjusted based on the current error of component d. Consequently, low frequency operation of sensor-less induction motor drive would be possible [9]. In [10], an FFVE-based sensor-less PMSM drive was developed with an improved Ljungberg-based rotor coupling flux monitor. Since the stator resistance, which is a highly significant parameter in low-speed performance, is not estimated, the sensor-less design performs poorly at low speeds. Although the Ljungberg observer used in [10] is powerful and reliable, it needs a larger number of observer gains, especially for estimating several parameters, compared to a simpler MRAS estimator, which has a comparative correction mechanism with fewer gains.

The main purpose of this study was to improve the low-speed performance of sensor-less speed control design based on feed forward voltage estimation (FFVE) for PMSM drive employed in electric vehicle drive which includes modified MRAS estimator and operates mathematically by continuously estimating the stator resistance and the rotor flux-linkage amplitude. While the stator inductance is set to its nominal value, the updated values in the feed forward voltage estimation model are used in the closed loop method. By estimating several MRAS parameters, the performance and stability of the sensor-less drive design at steady state and low speeds is notably improved.

Materials and Methods

The very first step in designing a closed loop control system, such as a model-reference adaptive system, is to identify and model the device. Without a precise model of the device, the design and analysis of the stability of the control system is not readily feasible, as the design of a controller is based on mitigating the unwanted features of the device while adding the desired features through the feedback control system. In addition, the controller parameters are adjusted according to the model, with the motive that in case the device parameters are indeterminate, the adaptive controllers provide a method for automatically adjusting the controller parameters. If the parameters of the device vary with time, adaptive control systems should be able to effectively respond to the desired performance. In this research, the model-reference adaptive system (MRAS) is used to control permanent magnet synchronous motor (PMSM) as the propulsion system of electric vehicles. In this method, the adverse effects of parameter change in speed control are reduced using stator feedforward voltage estimation (FFVE), which relies on the parameters of the motor. the stator resistance and the rotor flux-linkage are instantaneously estimated by an estimator and are continuously updated in the feed-forward voltage estimation mechanism using a closed-loop method. This method eliminates the sensitivity to parameter variations at low speeds. Furthermore, to improve the dynamics and overall stability of the system and eliminate transient fluctuations in speed estimation, a speed estimation method such as PLL is proposed, which is achieved by embedding a PI flow regulator in The q-axis and its output is obtained through a first-order filter by the FFVE method.

Dynamic model and steady state of PMSM

The dynamic dq model is used in the rotating synchronous reference framework for PMSM analysis with field-oriented control (FOC). The equations for PMSM stator voltage are presented in the rotating dq reference frame (rotor reference or synchronous reference) using Eqs. (1) and (2) and by eliminating the effects of magnetic field saturation and magnetic hysteresis.

$$v_q = i_q R_s + L_q \frac{di_q}{dt} + \left(\omega_e L_d i_d + \omega_e \lambda_f\right) \quad (1)$$

$$v_d = i_d R_s + L_d \frac{di_d}{dt} - \omega_e L_q i_q \quad (2)$$

where, $\boldsymbol{v_d}$, $\boldsymbol{v_q}$, $\boldsymbol{i_d}$and $\boldsymbol{i_q}$ are respectively the voltages and currents of the d and q components in the rotor reference frame. $\boldsymbol{R_s}$ is the resistance of the stator winding. $\boldsymbol{L_d}$ and $\boldsymbol{L_q}$ are the inductance of the d and q axes, respectively. $\boldsymbol{\omega_e}$is the angular (electrical) velocity of the rotor. $\boldsymbol{\lambda_f}$ is the flux-linkage given the constant magnetic rotor flux.

The steady state shape of the stator voltage equations on the dq axes can be obtained through the following equations by zeroing the derivative parts in Eqs. (1) and (2):

$$v_q = i_q R_s + \left(\omega_e L_d i_d + \omega_e \lambda_f\right) \quad (3)$$

$$v_d = i_d R_s - \omega_e L_q i_q \quad (4)$$

Estimating stator feedforward voltage

In this study, similar to the proposed method for controlling the sensor-less speed of an induction motor, stator voltage references $\boldsymbol{v_d^*}$ and $\boldsymbol{v_q^*}$ of stator are added to the PMSM steady state equation as feed forward estimating signals [11]

The current of the q-axis is controlled by the rotation speed or frequency of the stator voltage used in the q-axis coil. The voltage amplitude of the q-axis is obtained regardless of the derivative part, assuming that the actual currents approximately follow the reference values $\boldsymbol{i_q = i_q^*}$ and $\boldsymbol{i_d = i_d^*}$ (reference values are marked with * in the upper index while the estimated values are denoted by ^ (hat). The modified feedforward stator voltage equations for the proposed sensor-less speed control design in the dq reference frame are expressed as follows:

$$v_q^* = i_q^* \hat{R}_s + \left(\omega_e L_d i_d^* + \omega_e \hat{\lambda}_f\right) + K\Delta v \quad (5)$$

$$v_d^* = i_d^* \hat{R}_s - \omega_e L_q i_q^* + \Delta v \quad (6)$$

Where $\boldsymbol{\Delta v}$ is the output of the d axis of the PI current controller and $\boldsymbol{\omega_e}$is the electrical angular velocity for which the output of the q axis is the current controller. $\boldsymbol{\Delta v}$ is multiplied by the gain $\boldsymbol{\Delta v}$ and the voltage equation $\boldsymbol{v_q^*}$ is added to the q axis, which is expressed in the derivative section of the dynamic voltage equation presented in Equation (1). Similarly, the $\boldsymbol{v_q^*}$ term in Equation (5) acts as a derivative provided in Equation (2) to achieve a better transient response in sensor-less operation. Under dynamic conditions such as load disturbance, reference and parameter changes, a mismatch between the reference frame and the rotor flux vector produces non-zero terms, indicated by the voltage derivative section on the d-axis. This signal is the very same output of the d-axis current controller denoted by $\boldsymbol{\Delta v}$. Since the feed forward control $\boldsymbol{v_d^*}$ is defined by Equation (2) assuming a uniform field, this deviation produces a corrective signal through the $\boldsymbol{i_d}$ controller. Through gain K, this signal affects the reference q voltage ($\boldsymbol{v_q^*}$) along with the $\boldsymbol{i_q}$ current, causing the q-axis controller to reconstruct the reference frame current quickly or gradually with the purpose to correct the field [12], and thus the exact rotor speed is achieved.

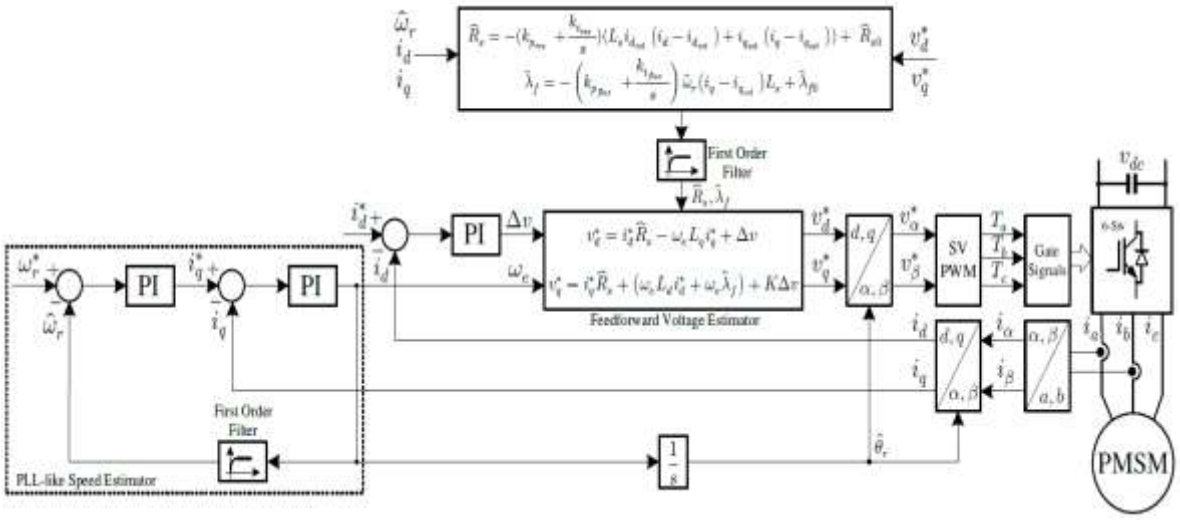

Figure 1: Block diagram of the proposed speed sensor model without sensor for PMSM based on MRAS estimation method

During steady-state operation, while the d axis current ($\boldsymbol{i_d}$) minimizes the flux-linkage error, the reference q axis current ($\boldsymbol{i_q}$) is obtained through the output of the speed controller and hence indirectly controls the torque. The rotor flux-linkage is defined proportional to the rate of change in $\boldsymbol{i_q}$ and is adjusted to make the d-axis current zero at steady state [13-14]. Therefore, the actual dq axis voltages will be proportional to the reference dq axis voltages. The output relationships of the d-axis current controller ($\boldsymbol{\Delta v}$) and the rotor flux-linkage ($\boldsymbol{\hat{\lambda}_f}$) in steady state when $\boldsymbol{i_d^* = 0}$ are obtained by altering equation (1) as follows:

$$v \approx \frac{\omega_e \hat{\lambda}_f}{K} \tag{7}$$

Which $\boldsymbol{\omega_e}$ is constant for the steady state. Therefore, the rotor flux-linkage ($\boldsymbol{\hat{\lambda}_f}$) is proportional to $\boldsymbol{\Delta v}$, which is approximated using the following equation:

$$\hat{\lambda}_f = \Delta v \tag{8}$$

Usually, a phase locked loop estimator with same position and speed is used to obtain the estimated rotor speed and position, which is done through the rotor estimate position error. The presence of a low-pass filter (LPF) in the PLL loop helps to improve the stability and compensates for the algebraic loop. The filter time constant depends on the mechanical properties of the whole system which strongly affects the dynamics and stability of the sensor-less control method.

Estimation of rotor flux-linkage and stator resistance based on MRAS method

In order to eliminate errors resulting from stator resistance change and rotor flux-linkage in PMSM sensor-less drive, multi-parameter estimation is performed using MRAS method. First, the MRAS parameter estimation equations are modified and hence employed to estimate the proposed feedforward stator voltage. The PMSM reference framework and customizable models that are presented in Equations (9) and (10), respectively, have subsequently been modified. Novel MRAS mathematical models are extracted to be used in the feedforward voltage estimation model.

The variables $\boldsymbol{K\Delta v}$ and $\boldsymbol{\Delta v}$ in the reference model are added to the structure of the proposed steady-state equations of PMSM. The modified MRAS equations have a linear feedforward model and a nonlinear feedback component that can be represented as follows:

$$\begin{bmatrix} \frac{di_q}{dt} \\ \frac{di_d}{dt} \end{bmatrix} = \begin{bmatrix} -\frac{R_s}{L_q} & -\frac{L_d}{L_q}\omega_e \\ \frac{L_q}{L_d}\omega_e & -\frac{R_s}{L_d} \end{bmatrix} \begin{bmatrix} i_q \\ i_d \end{bmatrix} + \begin{bmatrix} \frac{1}{L_q} & 0 \\ 0 & \frac{1}{L_d} \end{bmatrix} \begin{bmatrix} v_q \\ v_d \end{bmatrix} + \begin{bmatrix} -\frac{\lambda_f}{L_q}\omega_e \\ 0 \end{bmatrix} + \begin{bmatrix} -K\Delta v \\ -\Delta v \end{bmatrix} \quad (9)$$

Where $\widehat{\boldsymbol{R}}_{\boldsymbol{s}}$ and $\hat{\boldsymbol{\lambda}}_{\boldsymbol{f}}$ are respectively the estimated stator resistance and the estimated rotor flux-linkage, which are the outputs of the adaptive model. $\widehat{\boldsymbol{R}}_{\boldsymbol{s}}$ and $\hat{\boldsymbol{\lambda}}_{\boldsymbol{f}}$ are updated in the estimation block in the closed loop system. As a result, the estimated currents $\hat{\boldsymbol{\imath}}_{\boldsymbol{q}}$ and $\hat{\boldsymbol{\imath}}_{\boldsymbol{d}}$ are obtained as follows:

$$\begin{bmatrix} \frac{d\hat{\imath}_q}{dt} \\ \frac{d\hat{\imath}_d}{dt} \end{bmatrix} = \begin{bmatrix} -\frac{\hat{R}_s}{L_q} & -\frac{L_d}{L_q}\omega_e \\ \frac{L_q}{L_d}\omega_e & -\frac{\hat{R}_s}{L_d} \end{bmatrix} \begin{bmatrix} \hat{\imath}_q \\ \hat{\imath}_d \end{bmatrix} + \begin{bmatrix} \frac{1}{L_q} & 0 \\ 0 & \frac{1}{L_d} \end{bmatrix} \begin{bmatrix} v_q \\ v_d \end{bmatrix} + \begin{bmatrix} -\frac{\hat{\lambda}_f}{L_q}\omega_e \\ 0 \end{bmatrix} + \begin{bmatrix} -K\Delta v \\ -\Delta v \end{bmatrix} + \begin{bmatrix} G_1 & 0 \\ 0 & G_2 \end{bmatrix} \begin{bmatrix} i_q - \hat{\imath}_q \\ i_d - \hat{\imath}_d \end{bmatrix} \quad (10)$$

Where G is the observer gain matrix, $\boldsymbol{G_1}$ and $\boldsymbol{G_2}$ are the coefficients of the $\boldsymbol{G}$ matrix, which ensures that the linear feedforward model is positive and a real number. The selection of the exact values of the $\boldsymbol{G_1}$ and $\boldsymbol{G_2}$ coefficients presented in Equation (10) solves the algebraic loop problems that occur in laboratory studies.

Adaptive algorithms are usually realized through PI controllers. Therefore, the error of MRAS current estimator is presented in the following equation:

$$e = \begin{bmatrix} i_q - \hat{\imath}_q \\ i_d - \hat{\imath}_d \end{bmatrix} \quad (11)$$

Where errors $\boldsymbol{i_q - \hat{\imath}_q}$ and $\boldsymbol{i_d - \hat{\imath}_d}$ are adjusted using of PI control coefficients and according to Popov's inequality criterion. Therefore, two parameters of the error component are expressed as the following relation [15]:

The error correction is done with an adaptive model which is obtained by solving the nonlinear and linear feedforward models together, where in which $\widehat{\boldsymbol{A}} - \boldsymbol{A}$ and $\widehat{\boldsymbol{C}} - \boldsymbol{C}$ are used to achieve reference and estimated current and the outputs of the models. The adaptive equations for $\widehat{\boldsymbol{R}}_{\boldsymbol{s}}$ and $\hat{\boldsymbol{\lambda}}_{\boldsymbol{f}}$ are obtained through the following equations:

$$\hat{R}_s = -\left(k_{pres} + \frac{k_{ires}}{s}\right)\left(L_s\hat{\imath}_d(i_d - \hat{\imath}_d) + \hat{\imath}_q\left(i_q - \hat{\imath}_q\right)\right) + \hat{R}_{s0} \quad (12)$$

$$\hat{\lambda}_f = -\left(k_{pflux} + \frac{k_{iflux}}{s}\right)\omega_e\left(i_q - \hat{\imath}_q\right)L_s + \hat{\lambda}_{f0} \quad (13)$$

Where $\boldsymbol{k_{pres}}$ ،$\boldsymbol{k_{ires}}$ ،$\boldsymbol{k_{pflux}}$ ،$\boldsymbol{k_{iflux}}$ ،$\widehat{\boldsymbol{R}}_{\boldsymbol{s0}}$ and $\hat{\boldsymbol{\lambda}}_{\boldsymbol{f0}}$ are respectively, the proportional gain of the estimated resistance controller, the integral gain of the estimated resistance controller, the proportional gain of the estimated rotor flux-linkage, the integral gain of the estimated rotor flux-linkage, the initial estimated stator resistance and the initial estimated rotor flux-linkage. Estimated values for stator resistance and rotor flux-linkage offered in Equations (12) and (13) are guaranteed to produce a faster response than the closed loop cycle.

Stability analysis of current controller in dq axes

First, the open loop conversion function of the d-axis current loop is obtained without the PI controller, and then the zero of the d-axis PI current controller is used to eliminate the largest time constant of the open-loop conversion function. The design rules of the MO method for d-axis current control are approved. Stability analysis of the PI current controller in d axis is performed using Bode diagrams. The results of d-axis current control are obtained at a speed of 63 rpm under full load with parameter adjustment and without parameter adjustment. Under adjustment conditions, the stator resistance is 30% higher than the set nominal

value of the rotor flux-linkage and is set at 20% of its nominal value. The d-axis open loop flow controller is a 17-order system. A similar analysis is performed for the q-axis current loop, which is a 15-order system. The gain margin (GM) is 20.4 dB and the phase margin (PM) is 103° for unadjusted parameters. In the case of the adjusted parameter, the gain margin is 20.7 dB and the PM is 122°. According to the frequency domain stability criterion in both cases, the current control in q-axis is stable.

Stability analysis of sensor-less speed controller

In the open-loop speed control conversion function, the SO adjustment method is undertaken such that the small combined time constant pole with zero PI controller is eliminated. Hence, at least one of the poles of the open-loop velocity conversion function is located at or near the coordinate origin, and the phase margin is maximized by causing more delay in the system. Stability analysis of the sensor-less speed controller is performed at low speed (63 rpm) under full load for the conditions of the adjusted and unadjusted parameters using the bod diagram and the geometric roots and zeros.

The open loop Bode diagram of the speed controller is shown in Figure 4. At low frequencies, the phases higher than 180 degrees doesn't vary in the studied band, and hence it is not necessary to check the gain margin for both adjusted and unadjusted parameters.

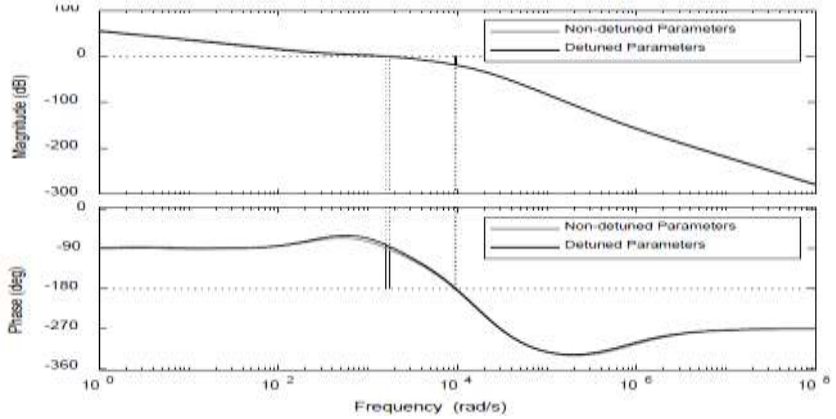

Figure 2: Bode diagram of d-axis current control for adjusted and unadjusted parameter conditions

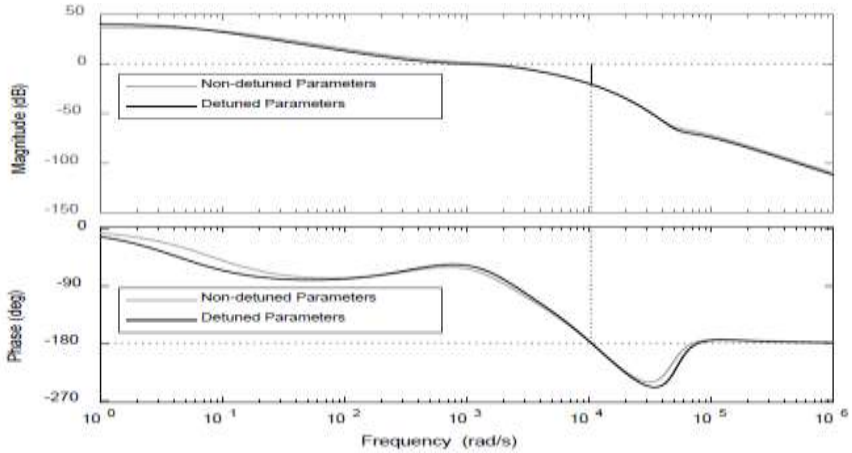

Figure 3: Bode diagram of q-axis current control for adjusted and unadjusted parameter conditions

The phase margin for unadjusted and adjusted parameters is 80.9 degrees and 80.6 degrees respectively. Therefore, frequency domain analysis of closed loop speed system indicates stability.

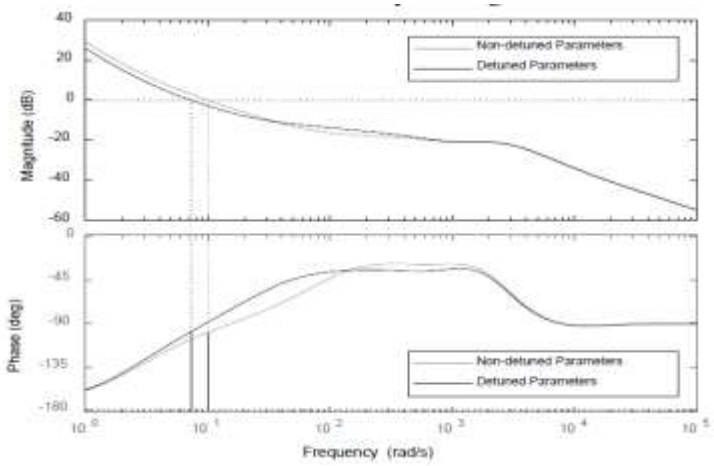

Figure 3: Bode diagram of speed control loop for adjusted and unadjusted parameter conditions

Mathematical modeling of electric vehicles

In order to control the electric vehicle, the equations of motion must be obtained. First, all the forces that affect the movement of the car must be analyzed. The equations must then be generated according to Newton's second law. All forces applied to the electric vehicle are shown in Figure 5. These forces are rotational resistance force ($\boldsymbol{F_{pe}}$) and ($\boldsymbol{F_{wg}}$), air resistance force ($\boldsymbol{F_{air}}$), engine thrust force ($\boldsymbol{F_{tr}}$), driving force ($\boldsymbol{F_{dr}}$), vehicle weight (G) and vertical surface force relative to the ground (N).

The resultant force is calculated as the driving force $\boldsymbol{F_{dr}}$ according to the following equations:

$$F_{dr} = F_{tr} - F_{pe} - F_{wg} - F_{air} \tag{14}$$

And

$$F_{pe} = \mu_d G \frac{d}{D} \tag{15}$$
$$F_{wg} = G \frac{2\delta}{D}$$
$$F_{air} = \frac{1}{2} A \rho \gamma v_{max}^2$$
$$F_{tr} = M_{max} \frac{k_{gr}}{r}$$
$$F_{dr} = ma$$
$$v = \int a dt$$
$$S = \int v dt$$

In which, $\boldsymbol{\mu_d}$ is the coefficient of friction between the pin and the bearing. **G**: vehicle weight, **d**: pin diameter, **D**: wheel diameter, δ: weight force displacement G in the direction of motion, **v**: vehicle speed, **A**: car front area, **ρ**: air density, **γ**: vehicle permeability coefficient, $\boldsymbol{M_{max}}$: maximum Engine torque, $\boldsymbol{v_{max}}$: maximum vehicle speed, **m**: vehicle mass, **a**: vehicle acceleration and **S**: vehicle location.

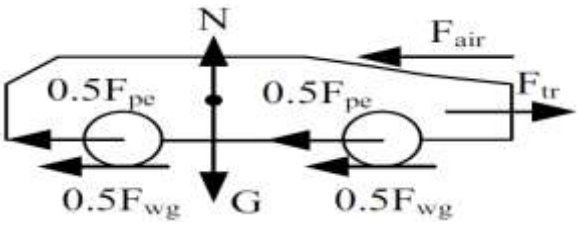

Figure 5: Forces applied to the electric vehicle

Results and Findings

Simulation of PMSM in an electric car with proposed MRAS design

The parameters and values for to the permanent magnet synchronous motor (PMSM) are presented in Table (1).

Table 1: Parameters of permanent magnet synchronous motor (PMSM)

PMSM engine parameters	Values
Stator resistance (R_s)	3.4Ω
Stator d-axis inductance (L_d)	$3.3\ mH$
Stator d-axis inductance (L_q)	$3.3\ mH$
Rotor magnetic flux-linkage (λ_f)	0.2961 $(v.s)$
Rotor inertia (J)	$0.0075\ Kg.m^2$
Number of poles (P)	4
Nominal voltage and frequency (V, f)	$230v, 60Hz$
Nominal power (P_n)	$1000w$
Nominal speed (N_n)	$900\ r.p.m$
Nominal load torque (τ_l)	$10\ N.M$

Also, various parameters related to MRAS controller and proportional and integral gains related to flux and torque comparators are listed in Table (2). The proposed system is implemented and simulated in the Simulink environment of MATLAB software.

Table 2: MRAS parameters

System parameters	values
Sampling time (T_s)	$100\mu s$
Base frequency (f_n)	$60\ Hz$
Switching frequency (f_{sw})	$10\ kHz$
DC link voltage	$565\ v$
Proportional gain of the flow controller	0.4970
Integral time constant of flow	$9.706 \times 10^{-4}(s)$
Integrated flow controller gain	512.0784
Proportional speed gain	0.2657
Time constant of speed integral	0.1238 (s)
Integral velocity gain	2.1468
Time constant of speed feedback	0.009 (s)
Time constant of current feedback	5×10^{-5} (s)
Feedforward gain	2.75

Simulation of PMSM at nominal speed and torque

The permanent magnet synchronous motor (PMSM), which is used as the driving force for a very light electric vehicle, rotates at a nominal speed of about 900 rpm and a nominal load torque of 10 Nm. The results of this simulation are shown in Figures (5) and (6).

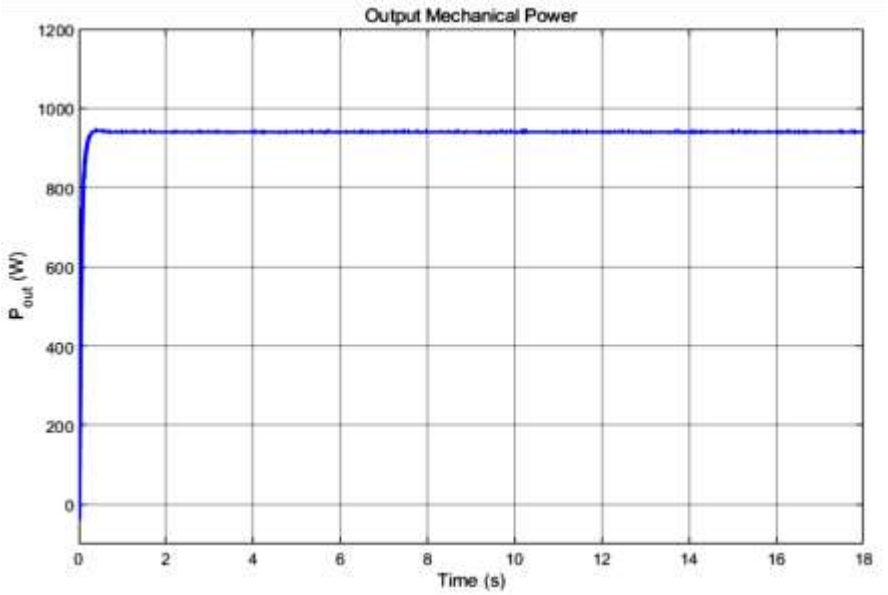

Figure 6: Mechanical power of PMSM under nominal speed of 900 rpm and nominal torque of 10 n-m

According to Figure 6, it can be seen that under the nominal conditions, the mechanical output power of the PMSM motor is about 950 watts. Figure 7 also shows the simulation of important parameters and quantities of the engine under the conditions of nominal speed and torque. It can be seen that the rotational speed of the motor corresponds exactly to the reference speed and the electromagnetic torque is exactly 10 Nm. Also under these conditions, the rotor junction flux is estimated to be 0.s16 V.s, while the stator resistance is about 12 ohms.

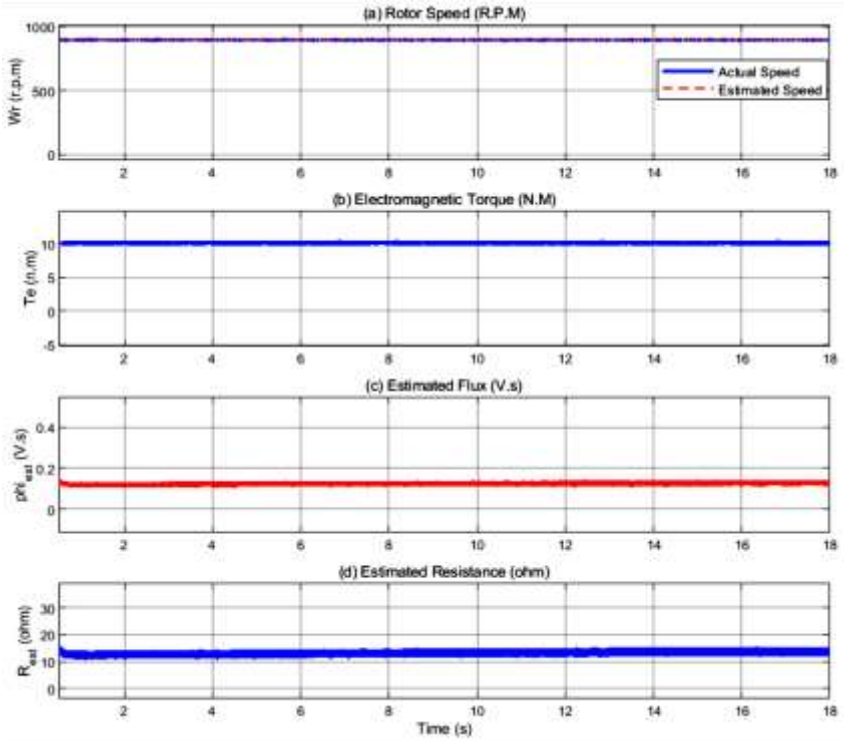

Figure 7: Simulation results of PMSM motor with MRAS sensor-less control method under nominal speed of 900 rpm and nominal torque of 10 n-m, (a) Motor speed (b) Electromagnetic torque (c) Estimated rotor flux-linkage (d) Estimated stator resistance

Simulation of PMSM motor at nominal torque and low speed (60 rpm) based on the proposed control method

In this part of the simulation, the capability of the PMSM motor is confirmed by the control method of estimating the improved MRAS parameter at low speeds. Under these conditions, a nominal torque of 10 Nm is applied to the motor and the reference speed is set at approximately 60 rpm. The corresponding simulation results are shown in Figures (8) and (9).

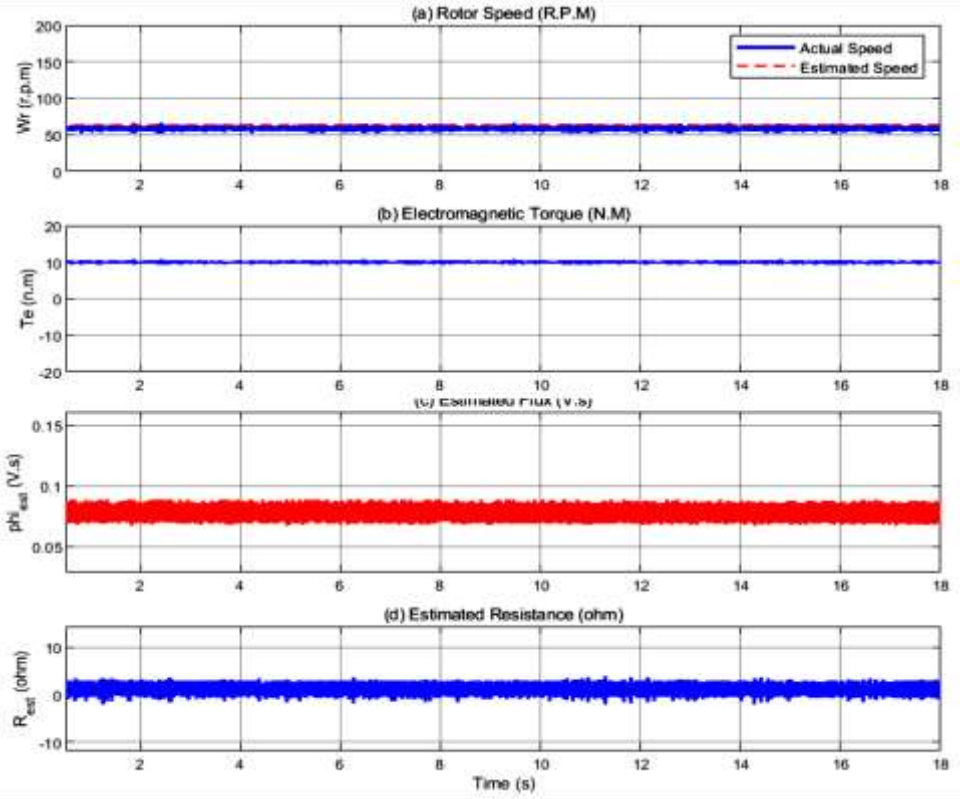

Figure 8: Simulation results of PMSM motor with MRAS sensor-less control method under 60 rpm speed and nominal torque of 10 n.m, (a) Motor speed (b) Electromagnetic torque (c) Estimated rotor flux-linkage (d) Estimated stator resistance

It can be seen from Figure 8 that there is some distortion in the rotor speed at low speeds. Also, the actual rotor speed is slightly lower than the reference speed resulting from the error of estimating the rotor flux and stator resistance. In these conditions, the amplitude of electromagnetic torque is exactly 10 nm and no specific ripple is observed. The estimated rotor flux ($\boldsymbol{\lambda_{est}}$) and the estimated stator resistance ($\boldsymbol{R_{est}}$) also have respectively mean values of 0.075 v.s and 2 ohms.

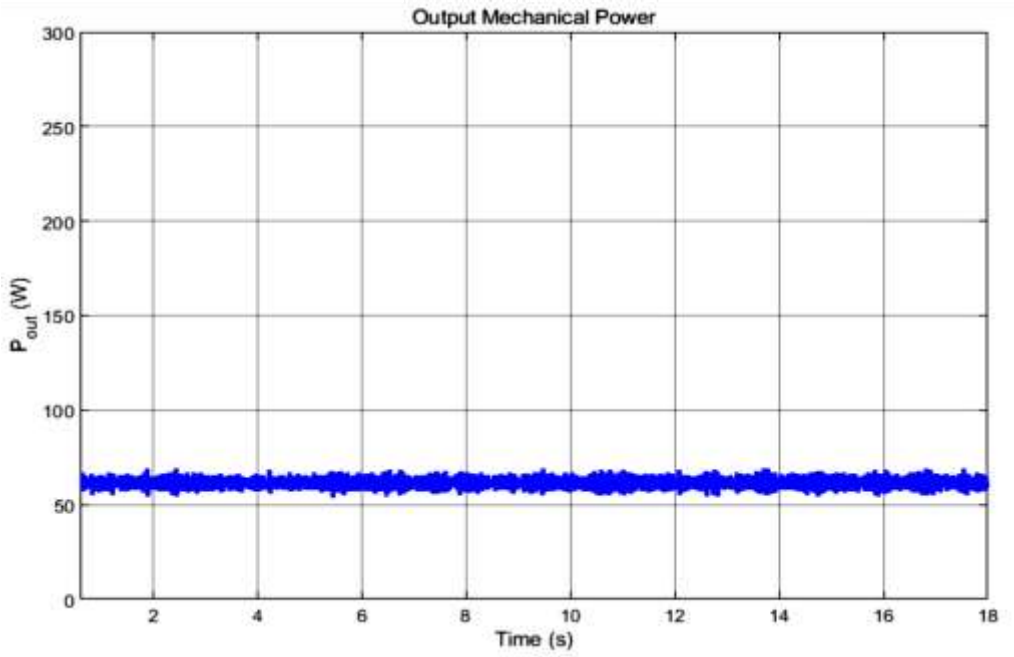

Figure 9: Mechanical power of PMSM motor under 60 rpm speed and nominal torque 10 nm

The mechanical output power of the PMSM motor at 60 rpm was estimates at 60 watts. Of course, in proportion to the speed waveform, which has some ripple, the output power waveform also has some oscillation and distortion, which is evident in Figure (4.4).

Conclusion

In this study, a permanent magnet synchronous motor (PMSM) using a sensor-less control strategy with multi-parameter MRAS estimation was employed in the propulsion system of a very light electric vehicle at the laboratory level. Simulation results were obtained for different modes of electric vehicle motion such as uniform motion, variable acceleration motion, etc., and the capability of the proposed control scheme was confirmed. The most significant results obtained from this analysis are as follows:

Compared to other sensor-less methods, the proposed MRAS method has an easy-to-implement yet powerful structure.

Since the sensor-less method is based on back EMF estimation, the effects of parameter variation from online multi-parameter MRAS estimation are highly nullified.

Because the MRAS is easier to develop than other parameter estimation methods, the feedforward voltage estimation does not impose too excessively high computational loads on the microprocessor.

Simulations were performed with the purpose of simultaneous estimation of stator resistance and rotor coupling flux. Moreover, it was observed that, similar to V/f control in induction motors, the FFVE sensor-less method allows starting from zero speed as much as possible, while maintaining stability at medium and nominal speeds under full load.

The presence of a low-pass filter in the phase-locked loop (PLL) helps to increase the stability and compensates for the algebraic loop. The filter time constant depends on the mechanical properties of the whole system, strongly affecting the dynamics and stability of the sensor-less control mechanism.

In the proposed MRAS, a low-pass filter (LPF) is employed to overcome the increase in the amount of linkage flux of the estimated rotor at low speed and when crossing zero, and compensates for the distortion effects caused by the estimation of the stator resistance. At low speeds when LPF is not adopted, the estimation values are small and the feed forward voltage estimation values are thus prone to error.

At lower speeds, there is some distortion in the rotor speed. Also, the actual rotor speed is slightly lower than the reference speed due to the error in estimating the rotor flux and stator resistance.

During deceleration, owing to the error of estimating the rotor junction flux whose amplitude is negative, an oscillation is evident in the speed and torque waveforms.

Based on the obtained results, for further studies in this field, it is suggested to employed the proposed MRAS control method to control the three-phase induction motor. It is also suggested that a method be adopted to eliminate PMSM motor current harmonics with the purpose of reduce losses in motor and thus improve efficiency.

References

[1] C. C. Chan, A. Bouscayrol, and K. Chen, "Electric, Hybrid, and Fuel-Cell Vehicles: Architectures and Modeling," IEEE Transactions on Vehicular Technology, vol. 59, pp. 589-598, 2010.

[2] L. Situ, "Electric Vehicle development: The past, present & future," in 2009 3rd International Conference on Power Electronics Systems and Applications (PESA), 2009, pp. 1-3

[3] K. T. Chau, C. C. Chan, and C. Liu, "Overview of Permanent-Magnet Brushless Drives for Electric and Hybrid Electric Vehicles," IEEE Transactions on Industrial Electronics, vol. 55, pp. 2246-2257, 2008

[4] Seok, Jul-Ki, Jong-Kun Lee, and Dong-Choon Lee. "Sensorless speed control of nonsalient permanent-magnet synchronous motor using rotor-position-tracking PI controller." IEEE Transactions on Industrial Electronics 53, no. 2 (2006): 399-405

[5] Deng, Weitao, Changliang Xia, Yan Yan, Qiang Geng, and Tingna Shi. "Online multiparameter identification of surface-mounted PMSM considering inverter disturbance voltage." IEEE Transactions on Energy Conversion 32, no. 1 (2016): 202-212.

[6] Dang, Dong Quang, Muhammad Saad Rafaq, Han Ho Choi, and Jin-Woo Jung. "Online parameter estimation technique for adaptive control applications of interior PM synchronous motor drives." IEEE Transactions on Industrial Electronics 63, no. 3 (2015): 1438-1449.

[7] Hamida, Mohamed Assaad, Jesus De Leon, Alain Glumineau, and Robert Boisliveau. "An adaptive interconnected observer for sensorless control of PM synchronous motors with online parameter identification." IEEE Transactions on Industrial Electronics 60, no. 2 (2012): 739-748.

[8] Yang, Chenguang, Tao Teng, Bin Xu, Zhijun Li, Jing Na, and Chun-Yi Su. "Global adaptive tracking control of robot manipulators using neural networks with finite-time learning convergence." International Journal of Control, Automation and Systems 15, no. 4 (2017): 1916-1924.

[9] Nagata, Koichiro, Toshiaki Okuyama, Haruo Nemoto, and Toshio Katayama. "A simple robust voltage control of high power sensorless induction motor drives with high start torque demand." IEEE Transactions on Industry Applications 44, no. 2 (2008): 604-611.

[10] Blasko, Vladimir, Luis Arnedo, and Dong Jiang. "An integral method combining V/Hz and vector control of permanent magnet motor." In 2014 IEEE Energy Conversion Congress and Exposition (ECCE), pp. 4472-4477. IEEE, 2014.

[11] Okuyama, Toshiaki, Noboru Fujimoto, Takayuki Matsui, and Yuzuru Kubota. "Vector control scheme of induction motor without speed and voltage sensors." IEEJ Transactions on Industry Applications 107, no. 2 (1987): 191-198.

[12] Holtz, Joachim. "Sensorless control of induction motor drives." Proceedings of the IEEE 90, no. 8 (2002): 1359-1394.

[13] Vukosavic, Slobodan N., and Aleksandar M. Stankovic. "Sensorless induction motor drive with a single DC-link current sensor and instantaneous active and reactive power feedback." IEEE Transactions on Industrial Electronics 48, no. 1 (2001): 195-204.

[14] Perng, Shyh-Shing, Yen-Shin Lai, and Chang-Huan Liu. "Sensorless control for induction motor drives based on new speed identification scheme." In Proceedings of Power Conversion Conference-PCC'97, vol. 2, pp. 553-558. IEEE, 1997

[15] Zhang, Xinan, and Gilbert Hock Beng Foo. "A constant switching frequency-based direct torque control method for interior permanent-magnet synchronous motor drives." IEEE/ASME Transactions on Mechatronics 21, no. 3 (2015): 1445-1456.